Cell Death and Differentiation (2011) 18, 282–292

www.nature.com/cdd

Bid-mediated mitochondrial damage is a key mechanism in glutamate-induced oxidative stress and AIF-dependent cell death in immortalized HT-22 hippocampal neurons

S Tobaben[1], J Grohm[1], A Seiler[2], M Conrad[2,4], N Plesnila[3] and C Culmsee*[,1]

Glutamate toxicity involves increases in intracellular calcium levels and enhanced formation of reactive oxygen species (ROS) causing neuronal dysfunction and death in acute and chronic neurodegenerative disorders. The molecular mechanisms mediating glutamate-induced ROS formation are, however, still poorly defined. Using a model system that lacks glutamate-operated calcium channels, we demonstrate that glutamate-induced acceleration of ROS levels occurs in two steps and is initiated by lipoxygenases (LOXs) and then significantly accelerated through Bid-dependent mitochondrial damage. The Bid-mediated secondary boost of ROS formation downstream of LOX activity further involves mitochondrial fragmentation and release of mitochondrial apoptosis-inducing factor (AIF) to the nucleus. These data imply that the activation of Bid is an essential step in amplifying glutamate-induced formation of lipid peroxides to irreversible mitochondrial damage associated with further enhanced free radical formation and AIF-dependent execution of cell death.
Cell Death and Differentiation (2011) **18,** 282–292; doi:10.1038/cdd.2010.92; published online 6 August 2010

Glutamate toxicity is a well-established cause for neuronal dysfunction and cell death in many acute and chronic neurological diseases. For example, increases in extracellular glutamate levels after acute brain damage by ischemic stroke, epilepsy or brain trauma may reach millimolar concentrations and induce massive Ca^{2+} influx and excitotoxic damage through activation of glutamate receptors such as *N*-methyl-D-aspartic acid (NMDA) receptors or α-amino-3-hydroxy-5-methyl-4-isoxazole-propionic acid (AMPA)/kainate receptors.[1,2] The initial increase in intracellular Ca^{2+} levels after stimulation of these glutamate receptors is rather short and the following molecular mechanisms of glutamate excitotoxicity in neurons are poorly defined. While inhibition of the glutamate-induced Ca^{2+} influx by NMDA-receptor antagonists or antagonists of AMPA/kainate receptors protected neurons from glutamate excitotoxicity in experimental settings, the therapeutic time window of such neuroprotective effects is limited *in vivo*, and (post-)treatment strategies with glutamate receptor antagonists have failed in clinical studies to date.[3,4] Therefore, understanding the mechanisms of glutamate toxicity beyond the initial stimulation of Ca^{2+} influx is of utmost importance to provide efficient strategies of neuroprotection by targeting sustained mechanisms of glutamate-induced neuronal cell death. Such mechanisms include, for example, increased formation of reactive oxygen species (ROS), the activation of apoptosis-related death signaling, mitochondrial damage and DNA degradation.

In particular, oxidative stress has been considered to cause neuronal dysfunction and cell death triggered by glutamate after acute brain injury and in age-related chronic neurodegenerative diseases. Therefore, recent research has focused on better understanding ROS formation and dissecting ROS-triggered neuronal death signaling pathways in order to identify novel therapeutic strategies against glutamate neurotoxicity. Under physiological conditions, cellular ROS levels are tightly controlled by low-molecular-weight radical scavengers and by a complex intracellular network of enzymes, such as catalases, superoxide dismutases Cu/Zn-SOD and Mn-SOD (SOD-2), and enzymes of the glutathione (GSH)- and thioredoxin-dependent families.[5,6] Under conditions of lethal stress associated with glutamate toxicity, that is, acute or chronic brain injury, these endogenous defense

[1]Institute for Pharmacology and Toxicology, Philipps University Marburg, Marburg, Germany; [2]Institute of Clinical Molecular Biology and Tumour Genetics, Helmholtz Zentrum München, Munich, Germany and [3]Department of Physiology, Royal College of Surgeons in Ireland (RCSI), Dublin, Ireland
*Corresponding author: C Culmsee, Institut für Pharmakologie und Toxikologie, Klinische Pharmazie, Philipps-Universität Marburg, Karl-von-Frisch-Str. 1, Marburg D-35033, Germany. Tel: +49 6421 2825780; Fax: +49 6421 2825720; E-mail: Culmsee@staff.uni-marburg.de
[4]Current address: German Center for Neurodegenerative Diseases (DZNE) and Helmholtz Center Munich, German Research Center for Environmental Health, Institute of Developmental Genetics, Ingolstädter Landstrasse 1, Neuherberg 85764, Germany.
Keywords: glutamate; neuronal cell death; apoptosis; mitochondria; lipid peroxidation; reactive oxygen species; apoptosis-inducing factor
Abbreviations: AIF, apoptosis-inducing factor; AMPA, α-amino-3-hydroxy-5-methyl-4-isoxazole-propionic acid; ANOVA, analysis of variance; BODIPY, 4,4-difluoro-5-(4-phenyl-1,3-butadienyl)-4-bora-3a,4a-diaza-s-indacene-3-undecanoic acid; COX, cyclooxygenase; DAPI, 4′,6-diamidino-2-phenylindole dihydrochloride; DCF, dichlorodihydrofluorescein-diacetate; FACS, fluorescence-activated cell sorting; FITC, fluorescein isothiocyanate; GSH, glutathione; GpX4, glutathione peroxidase 4; (12/15-)LOX, (12/15-)lipoxygenase; MTT, 3-(4,5-dimethylthiazol-2-yl)-2,5-diphenyltetrazolium bromide; NMDA, *N*-methyl-D-aspartic acid; NOX, NADPH-oxidase; OGD, oxygen glucose deprivation; PBS, phosphate-buffered saline; ROS, reactive oxygen species; SMAC/DIABLO, second mitochondria-derived activator of caspase/direct IAP binding protein with low pI; (Cu/Mn/Zn)-SOD, (copper/manganese/zinc)-superoxide dismutase; tBid, truncated Bid
Received 11.11.09; revised 01.6.10; accepted 25.6.10; Edited by L Greene; published online 06.8.10

systems fail to detoxify increasing ROS levels. Prominent sources of physiological intracellular ROS formation that may further be stimulated under conditions of cellular stress are, for example, lipoxygenases (LOXs), cyclooxygenases (COXs), NADPH-oxidases (NOXs) and the uncoupled mitochondrial respiratory chain.[7,8]

After exposure to glutamate, dysfunctional mitochondria may generate toxic amounts of intracellular ROS, which may further severely perturb cellular redox balance.[9] In addition, these organelles host pro-apoptotic proteins, for example, apoptosis-inducing factor (AIF), cytochrome *c* or SMAC/DIABLO (second mitochondria-derived activator of caspase/direct IAP binding protein with low pI), which may trigger caspase-dependent or caspase-independent death when released into the cytosol. Increasing evidence suggests a key role for mitochondrial AIF and related caspase-independent death in glutamate-induced neuronal death and in the injured adult brain.[10–12] In contrast to cytochrome *c*-mediated caspase-dependent cell death, AIF translocates to the nucleus and induces nuclear condensation, DNA fragmentation and cell death immediately after release from mitochondria.[13]

Neuronal HT-22 cells have been established as a suitable model system[14] to investigate glutamate-induced death signaling pathways that enhance ROS formation and lethal oxidative stress independent of NMDA-receptor stimulation, as these neuronal cells lack glutamate receptor expression and are thus not susceptible to glutamate-induced rapid calcium influx. Glutamate-induced death signaling in these cells involves GSH depletion and enhanced accumulation of ROS.[15] Our recent study identified GSH peroxidase 4 (GPx4) as an important mediator of oxidative stress-induced cell death pathway after GSH depletion.[16] Experimental GSH depletion or GPx4 disruption caused 12/15-lipoxygenase (12/15-LOX)-dependent lipid peroxidation, nuclear AIF translocation and cell death in fibroblasts. In the present study, we sought to address whether glutamate-induced cell death in HT-22 cells occurs through LOX-dependent lipid peroxidation and mitochondrial death signaling. Our results expose Bid as a key link between glutamate-induced activation of LOX and mitochondrial pathways of programmed cell death.

Results

Glutamate-induced oxidative stress in HT-22 cells involves lipid peroxidation by 12/15-LOX. Glutamate induces death in HT-22 immortalized hippocampal cells in a dose- and time-dependent manner (Figure 1a and b). Real-time recording of cellular impedance by the xCELLigence system and 3-(4,5-dimethylthiazol-2-yl)-2,5-diphenyltetrazolium bromide (MTT) assays revealed that cell death occurred 8–10 h after onset of exposure to 3 and 5 mM glutamate, and according to these measurements execution of cell death was concluded within 2–4 h, respectively.

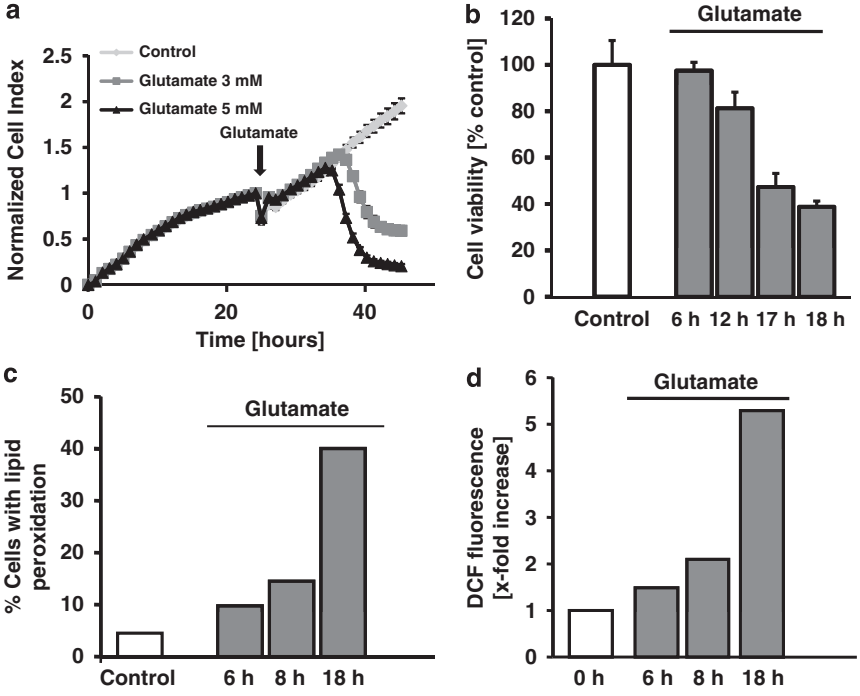

Figure 1 Glutamate leads to a time-dependent damage in HT-22 cells. (**a**) HT-22 cells were seeded in 96-well E-plates with a density of 4500 cells/well. Cells were observed for 48 h after seeding and treated with glutamate 5 mM after 24 h. Cell death became obvious 9–10 h after glutamate challenge. After onset of cell death HT-22 cells died within 3–5 h ($n=8$). (**b**) Cells were treated with glutamate at concentrations of 5 mM for 6, 12, 17 and 18 h. Cell death was detected by MTT assay ($n=8$). (**c**) Glutamate induces the production of lipid peroxides. Glutamate treatment was performed for 6–17 h. After addition of 2 μM BODIPY 581/591 C11 for 60 min, quantification was done by FACS analysis. Following glutamate exposure, a twofold increase in lipid peroxides after 6–8 h, and a secondary boost could be detected after 18 h ($n=3$). (**d**) Glutamate leads to formation of ROS and supports the production of lipid peroxides. Glutamate was added to the cells at a concentration of 3 mM. ROS levels were detected by dichlorodihydrofluorescein-diacetate (DCF) and quantified by FACS analysis ($n=3$). (**a–d**) All experiments were repeated at least three times and results are reported as mean ± S.D.

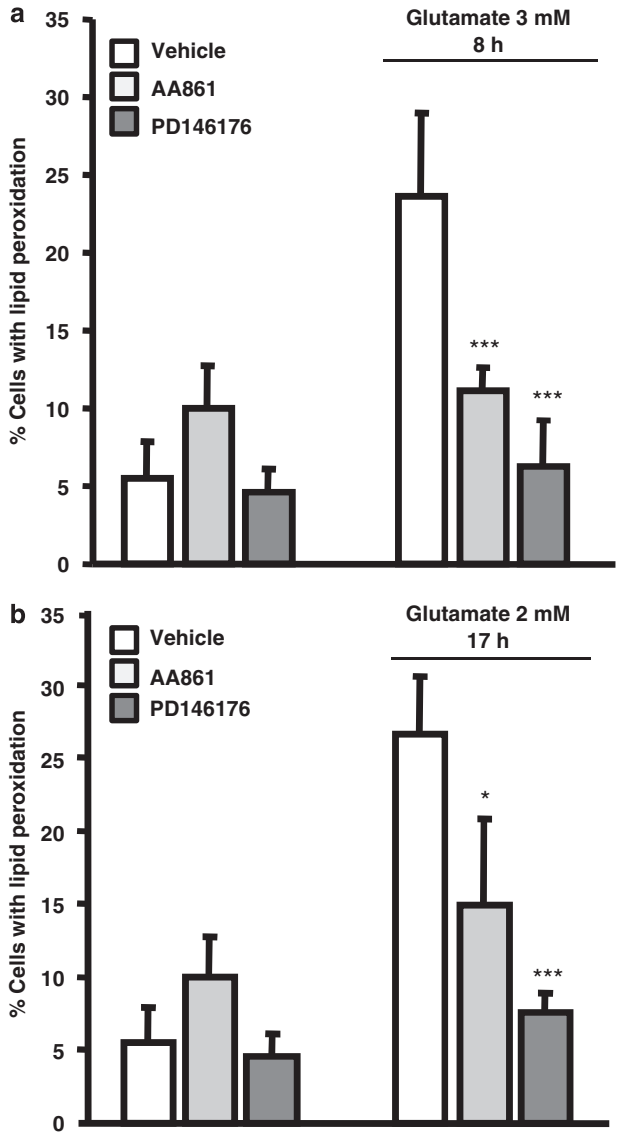

Figure 2 LOX inhibitors prevent peroxide formation in HT cells exposed to glutamate. Lipid peroxidation was detected 8 h (**a**) and up to 17 h (**b**) after onset of glutamate exposure by FACS analysis after staining of cells with BODIPY C11 (Ex = 488 nm, Em = 530 nm, 613 nm). The LOX inhibitor AA861 (0.1 μM) or PD146176 (0.5 μM) was added 1 h before the glutamate challenge ($n = 3$). (**a, b**) All experiments were repeated three times and the results represent the mean ± S.D. $^*P < 0.05$, $^{***}P < 0.001$ compared with glutamate-treated cells (ANOVA, Scheffé-test)

As detected by the fluorescent dye BODIPY (4,4-difluoro-5-(4-phenyl-1,3-butadienyl)-4-bora-3a,4a-diaza-s-indacene-3-undecanoic acid) and fluorescence-activated cell sorting (FACS) analyses, glutamate-induced cell death was accompanied by an accumulation of lipid peroxides. Notably, lipid peroxidation appeared to be moderate, that is, up to twofold, within 6–8 h of glutamate exposure, followed by a more pronounced, secondary increase within 8–18 h after glutamate treatment (Figure 1c). Measurements with dichlorodihydrofluorescein-diacetate (DCF) confirmed a nearly twofold increase in ROS formation 6–8 h after glutamate treatment, followed by a secondary boost of ROS formation at 18 h after the glutamate challenge (Figure 1d).

To identify the source of lipid peroxidation, we tested the effect of LOX inhibitors in our current model system. As illustrated in Figure 2a, the LOX inhibitors PD146176 and AA861 prevented the first glutamate-induced increase in lipid peroxidation after 6–8 h. In addition, LOX inhibition significantly attenuated the boost of lipid peroxides detected at 17 h after onset of glutamate treatment (Figure 2b). For these experiments, two different glutamate concentrations were applied to demonstrate the effects of LOX inhibitors on glutamate-induced lipid peroxidation. For induction of substantial amounts of lipid peroxides at early time points, that is, within 8 h after the onset of glutamate treatment, we applied 3 mM glutamate (Figure 2a), whereas 2 mM glutamate was used for the long-term end point (17 h, Figure 2b), because at glutamate concentrations higher than 3 mM the cells were severely damaged at the later time point and could not be used for subsequent BODIPY loading and FACS analyses.

The LOX inhibitor PD146176 significantly prevented glutamate-induced cell death in a concentration-dependent manner. Notably, PD146176 fully protected HT-22 cells against glutamate toxicity at a concentration of 0.5 μM (Figure 3a and c) and significantly reduced the annexin-V/propidium iodide-positive cells (Figure 3b). Comparable results were obtained by using the LOX inhibitor AA861 (Supplementary Figure 1), and the anti-oxidants *N*-acetyl cysteine and Trolox (Supplementary Figure 2a and b). In contrast, the COX inhibitor indomethacin (5–100 μM) failed to protect the cells against glutamate toxicity (Figure 3d). These findings demonstrate that LOX, but not COX, has a major role in oxidative stress-induced cell death after glutamate exposure in HT-22 cells. In primary neurons, it has been suggested that glutamate-induced excitotoxicity involved both disruption of the intracellular Ca^{2+} homeostasis and increased oxidative stress. Here, we investigated the effect of PD146176 in glutamate-induced cell death in primary cortical neurons. The 12/15-LOX inhibitor PD146176 significantly reduced cell death in primary neurons (Figure 3e). Further, primary neuronal cultures from Alox15-mice (15-LOX knockout mice) were significantly protected from glutamate toxicity compared with wild-type cultures (Figure 3f). These results strongly suggest that activation of 12/15-LOX has an important role in both model systems of glutamate toxicity, that is, in glutamate-induced oxytosis in HT-22 cells and in excitotoxic cell death in primary neurons.

We next determined the protective time window of LOX-dependent lethal oxidative stress in neuronal cell death and added the 12/15-LOX inhibitor PD146176 at different time points between 2 and 15 h after the onset of glutamate treatment. HT-22 cells were protected against glutamate toxicity even when PD146176 was added up to 8 h after the glutamate challenge (Figure 4a), indicating that beyond that time point glutamate-induced cell death proceeded too far for protection by LOX inhibition. Similar results were obtained with Trolox, which also protected the cells against glutamate toxicity with a similar post-treatment time window of 8 h (Figure 4b).

12/15-LOX inhibitor PD146176 protects against glutamate-induced mitochondrial fission and prevents AIF translocation to the nucleus. Glutamate-induced cell death in neurons involves mitochondrial damage and release

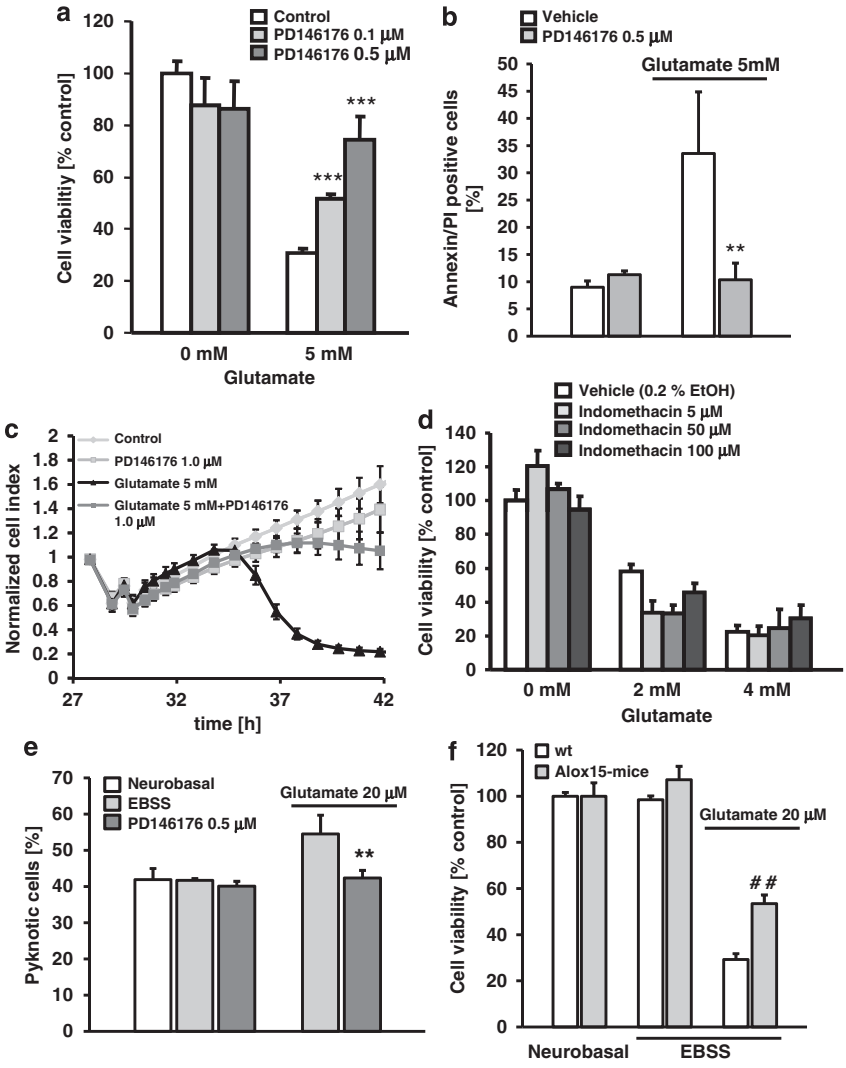

Figure 3 LOX inhibitors protect HT-22 cells against glutamate-induced cell death. (**a**) The LOX inhibitor PD146176 was applied 1 h before exposure to glutamate (5 mM) at concentrations of 0.1 and 0.5 μM. MTT ($n=8$) assay and FACS analysis were used to determine cell viability 18 h after onset of glutamate treatment. (**b**) LOX inhibitor PD146176 reduced the number of annexin-V/propidium iodide-positive cells compared with glutamate treated cells significantly. Cells were pretreated with the 12/15-LOX inhibitor PD146176 (0.5 μM) 1 h before glutamate challenge (5 mM). Cells were stained with annexin-V and propidium iodide and detected with FACS analysis ($n=4$). (**c**) HT-22 cells were seeded in 96-well E-plates with a density of 4500 cells/well. Cells were pretreated with PD146176 for 1 h and treated with glutamate 5 mM after 24 h ($n=8$). (**d**) The COX inhibitor indomethacin does not protect HT-22 cells against cell death induced by glutamate treatment. Indomethacin (5–100 μM) was added 1 h before exposure to glutamate at indicated concentrations. MTT assay was used to determine cell viability 18 h after glutamate treatment ($n=8$). (**e**) PD146176 protects primary cortical neurons against glutamate-induced cell death. Primary cortical neurons were pretreated with PD146176 0.5 μM 1 h before adding glutamate (20 μM). After 18 h cells were fixed with paraformaldehyde (4%) and stained with DAPI. The percentage of pyknotic nuclei was evaluated by counting 200 living and pyknotic cells per cell culture dish ($n=5$). (**f**) Primary cortical neurons were prepared from Alox-15 and wild-type mice at embryonic day E16. Cells were treated on day 6 in culture with glutamate (20 μM). Cell death was significantly reduced in Alox15 cultures compared with wild-type neurons. Cell death was evaluated by counting 200 DAPI-stained cells per dish ($n=5$). All data are provided as mean ± S.D. $^{**}P<0.01$, $^{***}P<0.001$ compared with glutamate-treated cells and $^{\#\#}P<0.01$ compared with glutamate-treated wild-type neurons (ANOVA, Scheffé test)

of pro-apoptotic mitochondrial proteins such as AIF.[10,13] Further, the time pattern of the increase in lethal oxidative stress after glutamate exposure indicated LOX-dependent induction of cell death signaling upstream of mitochondria. Therefore, we next investigated whether 12/15-LOX inhibition was also sufficient to prevent the hallmarks of mitochondrial damage, such as mitochondrial fission and translocation of AIF from mitochondria to the nucleus. After glutamate treatment, most cells showed significant fragmentation of the mitochondria appearing as small round organelles in the damaged cells in contrast to long tubular mitochondria observed under control conditions (Figure 5a and b). The 12/15-LOX inhibitor PD146176 preserved the mitochondrial morphology despite glutamate exposure, and in cells co-treated with the inhibitor the mitochondria appeared as a network of long tubular organelles similar to controls (Figure 5a). As these data implied preserved mitochondrial integrity, we next explored the effect of PD146176 on AIF release from mitochondria after glutamate challenge. AIF translocation has been identified as the final step of caspase-independent mitochondrial death signaling in neurons.[10,13] In line with

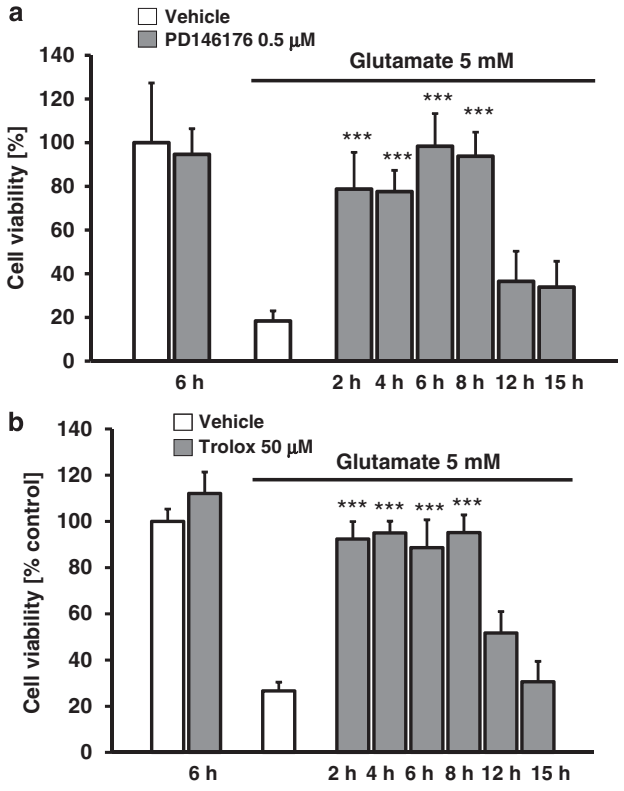

Figure 4 (**a**) LOX inhibitor PD146176 protects HT-22 cells when applied up to 8 h after glutamate treatment. The Lox inhibitor PD146176 was added at time points between 2 and 15 h after onset of glutamate treatment (5 mM). MTT assay was used to determine cell viability 18 h after onset of glutamate exposure ($n = 8$). (**b**) Trolox protects HT-22 cells against glutamate toxicity when applied up to 8 h after glutamate challenge. Cells were treated with Trolox (50 μM) at time points between 2 and 15 h after glutamate (5 mM) challenge. Cell viability was detected by MTT assay ($n = 8$). (**a**, **b**) All experiments were repeated three times and the results indicate the mean ± S.D. ***$P < 0.001$ compared with glutamate-treated cells (ANOVA, Scheffé-test)

these earlier findings, HT-22 cells immunostained for AIF clearly showed AIF relocation and cell death at 18 h after the glutamate challenge. 12/15-LOX inhibition by PD146176 prevented AIF translocation to the nucleus and preserved cell morphology (Figure 5c). These findings were confirmed by western blot analysis, as AIF was upregulated by 33% over the control level following glutamate treatment, whereas PD146176 could avert glutamate-induced AIF relocation (Figure 5d). These data further support a role for 12/15-LOX activity upstream of mitochondrial release of AIF to the nucleus.

The small-molecule Bidinhibitor BI-6C9 attenuates glutamate-induced oxidative stress. Recently, we reported a major role for the pro-apoptotic BH3-only protein Bid in mitochondrial demise upstream of AIF-mediated execution of caspase-independent death in neuronal cells exposed to glutamate.[10,13] Here, we further investigated whether pro-apoptotic activation of Bid occurred upstream of LOX-dependent lipid peroxidation and related cell death mechanisms. Measuring lipid peroxidation by BODIPY staining and FACS analysis revealed that Bid inhibition did not affect early increases in lipid peroxidation within 6–8 h after glutamate treatment, thus excluding direct radical scavenger activities of the Bid inhibitor (Figure 6a). Notably, BI-6C9 significantly reduced the pronounced accumulation of lipid peroxides that was associated with cell death in the vehicle-treated controls at 17 h after glutamate exposure (Figure 6b), and the Bid inhibitor also significantly protected HT-22 cells against the glutamate challenge up to control levels, confirming the important role of Bid in glutamate-induced neuronal cell death (Figure 6c). These data indicate that the initial increase in LOX-dependent lipid peroxidation at 6–8 h occurs upstream of Bid activation and is not affected by the Bid inhibitor. However, Bid activation seems to be an important link between the primary increase in lipid peroxides and the secondary boost of lipid peroxides, which marks the 'point of no return' that includes fatal mitochondrial damage and AIF-dependent execution of cell death. Notably, we could not detect Bid cleavage in the HT-22 cells, indicating either only a very small amount of Bid cleavage or a different way of Bid activation that involved mitochondrial translocation of full-length Bid independent of caspase-8 cleavage as recently described (Figure 6d).[13,17]

This role for Bid as an essential link between initial oxidative stress mediated by enhanced LOX activity and the secondary boost of lipid peroxidation associated with Bid-induced demise of mitochondrial function was further addressed using a truncated Bid (tBid) expression vector. The transfection of HT-22 cells with tBid induced significant cell death compared with cells transfected with the control plasmid (Figure 7a). In contrast to BI-6C9, both LOX inhibitors PD146176 and AA861 failed to protect the cells against tBid toxicity. It is important to note that over-expression of tBid may only partly reflect the mechanism of Bid-mediated death signaling, as Bid cleavage could not be detected in HT-22 cells after the glutamate challenge. However, BI-6C9 prevented both translocation of full-length Bid to mitochondria and tBid-mediated AIF release and cell death, suggesting that this model system is appropriate to mimic the mechanisms mediating Bid neurotoxicity.[13] In addition, the vitamin E analogue Trolox, an established antioxidant acting on lipid peroxides, could not prevent tBid-induced cell death, while glutamate-induced cell death was entirely abrogated (Figure 7b). These data strongly suggest that lipid peroxidation occurs upstream of Bid activation, whereas tBid-induced mitochondrial demise and the associated execution of cell death cannot be attenuated by radical scavengers or LOX inhibitors.

Discussion

In the present study we identify an important role for Bid acting as a key link between early ROS formation by 12/15-LOX and downstream mitochondrial damage and release of mitochondrial AIF to the nucleus that executes cell death after glutamate challenge in neuronal cells. In this model system of HT-22 cells, glutamate induces lethal oxidative stress independently of glutamate receptor-mediated calcium influx by inhibition of cysteine import through system xc-inhibition[18] and subsequent depletion of intracellular GSH levels.[15] GSH depletion leads to enhanced lipid peroxidation and eventually cell death mediated by the activation of LOX but not by COXs.

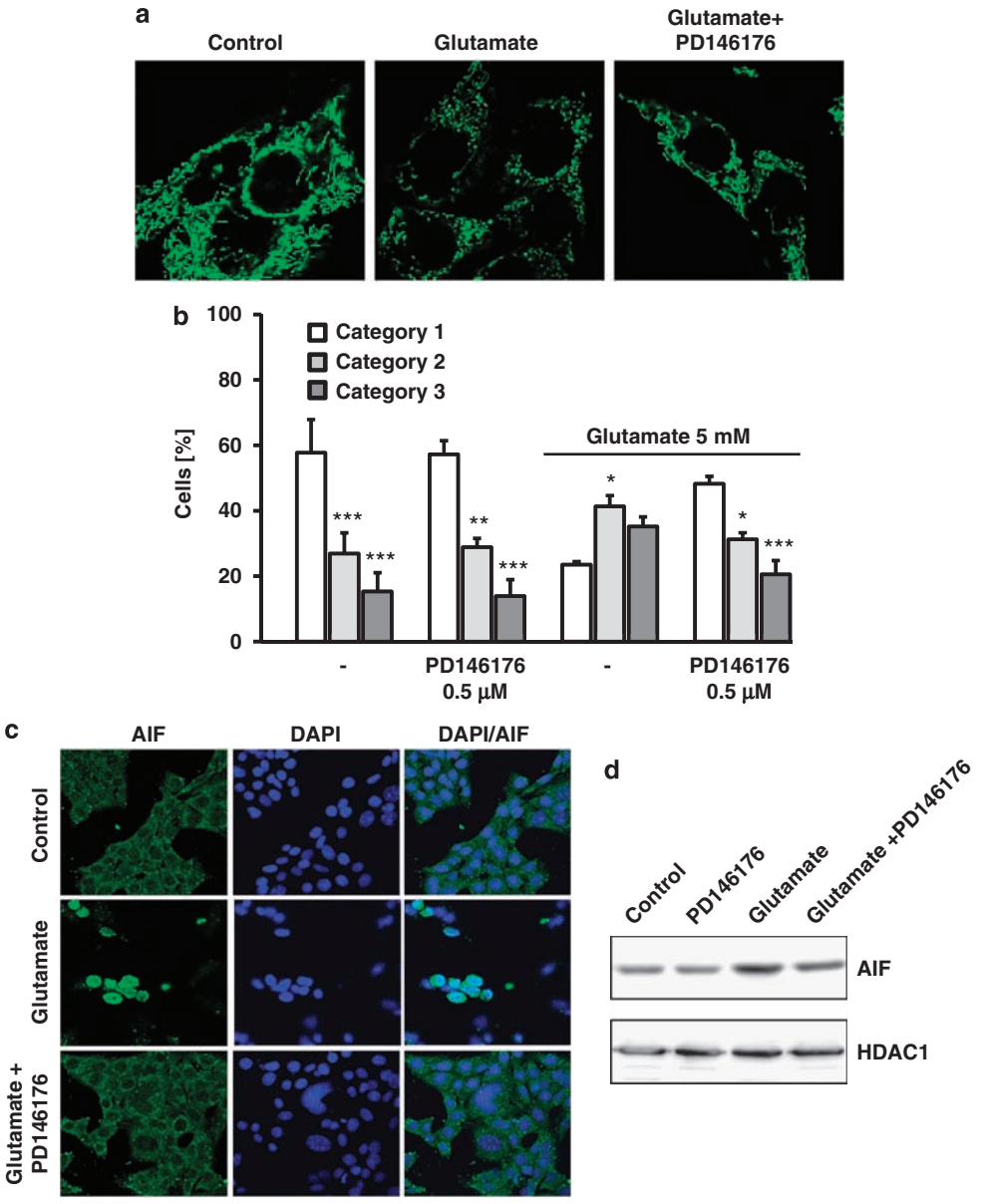

Figure 5 LOX inhibitor PD146176 0.5 μM prevents mitochondrial fragmentation and AIF-translocation to the nucleus. (**a**) HT-22 cells were transfected with mitoGFP using Lipofectamine 2000. After 24 h, the cells were damaged with glutamate 5 mM ($n=4$). (**b**) Mitochondrial morphology was analyzed by fluorescence microscopy and classified into three categories indicating the status of fission and fusion (category 1: tubulin-like, category 2: intermediate, category 3: fragmented) ($n=4$). (**c**) HT-22 cells were treated with glutamate 5 mM 24 h after seeding. PD146176 (0.5 μM) was applied 1 h before glutamate. Cells were fixed and immunostained 18 h after the treatment. Nuclei were stained with DAPI. Pictures were taken with a confocal microscope. The 12/15-LOX inhibitor prevented translocation of AIF to the nucleus. (**d**) HT-22 cells were damaged with glutamate and treated with PD146176 as indicated. After 14 h nuclear extracts were obtained for western blot analyses of AIF. HDAC1 served as a loading control ($n=3$). (**a**–**d**) All experiments were repeated at least three times and all data are provided as mean ± S.D. $^{*}P<0.05$, $^{**}P<0.01$, $^{***}P<0.001$ compared with glutamate-treated cells (ANOVA, Scheffé test)

Accordingly, only the 12/15-LOX inhibitors, but not the general COX inhibitor indomethacin, rescued HT22 cells from glutamate-induced cell death. In a recent study, we identified the functional loss of Gpx4 as the underlying mechanism that links reduced GSH levels to increases in lipid peroxidation by 12/15-LOX.[16] In an inducible Gpx4 knockout fibroblast system, we unraveled that loss of GPx4 sparks 12/15-LOX-derived lipid peroxidation and subsequent execution of caspase-independent cell death by mitochondrial release of AIF. Here, we show that glutamate-induced GSH deprivation in neuronal cells triggers LOX-dependent lipid peroxidation that contributes to the essential steps of glutamate-induced cell death. The 12/15-LOX inhibitors prevented the initial moderate rise in lipid peroxidation and consequently protected cells from further ROS-mediated cell death signaling triggered by glutamate. The central role for increased lipid peroxide generation in glutamate-mediated neuronal cell death was further substantiated by using the radical

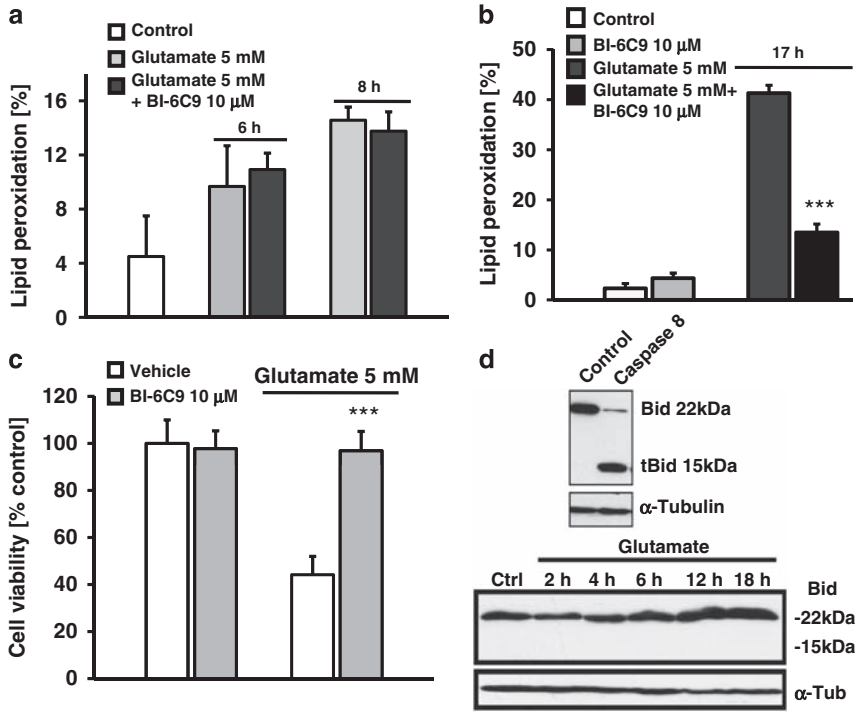

Figure 6 Bid inhibitor BI-6C9 protects cells against glutamate toxicity and prevents the secondary boost of ROS formation. Lipid peroxidation was detected 6–8 h (**a**) and up to 17 h (**b**) after onset of glutamate exposure by FACS analysis after staining cells with BODIPY C11 (Ex = 488 nm, Em = 530 and 613 nm). The Bid inhibitor BI-6C9 was present in the medium 1 h before and during the glutamate challenge ($n = 3$). (**c**) HT-22 cells were damaged with glutamate (5 mM) and BI-6C9 (10 μM). Cell viability was detected by MTT assay 18 h after the onset of glutamate treatment ($n = 8$). All experiments were repeated three times and the results indicate the mean ± S.D. ***$P < 0.001$compared with glutamate-treated cells (ANOVA, Scheffé test). (**d**) Glutamate does not induce Bid cleavage in HT-22 cells. HT-22 cells were treated with glutamate for 2–18 h. To test whether the anti-Bid antibody could detect full-length Bid as well as tBid, control cell extracts were incubated with recombinant caspase-8 *in vitro* before performing the indicated immunoblot detection (upper panel). In contrast to caspase-8-incubated cell extracts, protein extracts from HT-22 cells exposed to glutamate did not reveal Bid cleavage at the indicated time points (lower panel)

scavengers Trolox and *N*-acetylcysteine, which efficiently protected the HT-22 cells when applied within a time window of 8 h.

Both reduced GSH levels and increased ROS formation are established mechanisms that contribute to neuronal death in models of chronic and acute neurodegeneration.[19–21] Thus, the present finding in HT-22 cells showing a prominent role of 12/15-LOX for ROS formation in glutamate-induced cell death is relevant for mechanisms underlying neuronal injury and death in neurodegenerative diseases and after acute brain damage, such as trauma and stroke, where extracellular glutamate levels significantly increase after the respective injury. In addition, experiments in primary neurons also confirmed a major role for LOX-dependent mechanisms in glutamate-induced neuronal cell death in the presence of glutamate receptor ion channels. In these primary cells the LOX inhibitor PD146176 did not prevent the initial short increase in $(Ca^{2+})_i$ after glutamate exposure, but significantly attenuated the secondary sustained increase in intracellular calcium levels and cell death (data not shown). These findings support the conclusion that the LOX inhibitors interfered with delayed downstream execution mechanisms of glutamate neurotoxicity, such as ROS formation, sustained increases in $[Ca^{2+}]_i$ and mitochondrial damage. Thus, lipoxygenases are promising targets for therapeutic strategies against glutamate-mediated death signaling that may occur in the presence or absence of glutamate receptor ion channels. It is important to note that NOX inhibition also protected against cell death in the present model system, suggesting that NOX also contributes to glutamate neurotoxicity (Supplementary Figure 3). This finding supplements recent reports indicating that NOX activation links NMDA-receptor-mediated increases in $(Ca)_i$ levels and ROS formation.[7] Our data now suggest that NOX activity is also involved in glutamate-induced ROS formation and cell death in the absence of NMDA receptors and independent of increased $(Ca)_i$.

It is interesting to note that ROS formation after glutamate exposure of HT-22 cells apparently occurred in a biphasic manner. We observed initial moderate increases in lipid peroxidation within 6–8 h followed by a boost of lipid peroxides detectable up to 18 h after glutamate administration. Whereas the 12/15-LOX inhibitors fully abrogated the lipid peroxide accumulation, pharmacological inhibition of the pro-apoptotic BH3-only death protein Bid only impeded sustained increase in lipid peroxides but did not interfere with the initial ROS formation within the first 8 h. In contrast to recent data suggesting a potential role of LOX alone for the release of cytochrome *c* in isolated mitochondria,[22] our present findings in intact cells reveal a crucial role for Bid that is required for mitochondrial execution of cell death after the initial formation of lipid peroxides. Bid has been revealed as a key mediator of

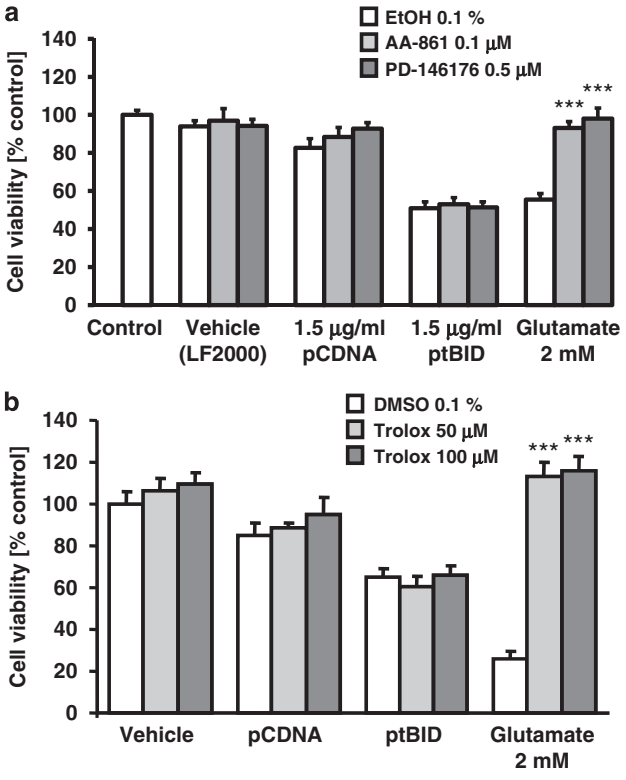

Figure 7 LOX inhibitors or Trolox does not attenuate the cytotoxic effect of tBid. (**a**) PD146176 (0.5 μM) and AA861 (0.1 μM) were added to HT-22 cells before transfection with tBid. Cell death was detected by using MTT assay 14 h after the transfection ($n=3$). (**b**) The vitamin E analog Trolox (50, 100 μM) was applied before transfection of HT-22 cells with tBid or exposure to glutamate. MTT assay was used to determine cell viability 24 h later ($n=3$). (**a**, **b**) All experiments were repeated three times and the results are reported as mean $\pm$ S.D. ***$P<0.001$ compared with glutamate-treated cells (ANOVA, Scheffé test)

cell death in different paradigms of neurodegeneration, including model systems of oxidative stress and excitotoxicity *in vitro*, and cerebral ischemia and brain trauma *in vivo*.[23] Accordingly, Bid knockout mice developed significantly reduced brain damage after cerebral ischemia[24,25] and brain trauma.[26] Similar neuroprotective results were obtained in cultured neurons from Bid-deficient mice when exposed to oxygen glucose deprivation (OGD).[24] Further, small-molecule inhibitors of Bid provided protective effects against glutamate-induced excitotoxicity or OGD in cultured primary neurons[10,27] and prevented mitochondrial demise, AIF release and cell death in HT-22 cells exposed to oxidative stress induced by glutamate or amyloid-beta peptide.[13] These different paradigms of lethal stress induce activation of Bid, which translocates to the mitochondria, where it mediates mitochondrial membrane permeabilization and release of death proteins such as cytochrome *c* or AIF.[17,28] Therefore, Bid activation is a common feature of death signaling that can significantly amplify deadly stress signals through involvement of mitochondrial mechanisms in the execution of cell death.

Indeed, the proposed timing of transition from moderate to severe oxidative stress fits well with the timing of Bid translocation to mitochondria and indicators of mitochondrial damage such as loss of mitochondrial membrane potential and subsequent release of AIF as determined in our previous work.[13] These findings suggest a transition phase wherein Bid acts as a crucial link between the 12/15-LOX-dependent initial increases in lipid peroxidation and the following mitochondrial damage. This conclusion is supported by our previous finding that the small-molecule Bid inhibitor BI-6C9 or Bid siRNA prevented mitochondrial damage, AIF translocation and cell death in neurons.[13] Moreover, the therapeutic time window of 8–10 h identified in our previous study for the Bid inhibitor is in accordance with the 'point of no return' and the associated secondary boost of oxidative stress revealed in the present study. Here, the LOX inhibitor PD146176 showed a similar therapeutic time window of approximately 8 h after onset of the glutamate challenge. This supports the view that accumulating oxidative stress leads to Bid-mediated mitochondrial damage, which marks the execution phase of cell death that cannot be blocked by LOX inhibitors or radical scavengers targeting the initiation phase.

The essential role for Bid mediating mitochondrial dysfunction and cell death downstream of 12/15-LOX activation in the present model of oxidative stress was further confirmed using tBid expression constructs that induce cell death by immediate mitochondrial translocation of tBid and subsequent induction of mitochondrial damage.[28,29] In this paradigm, only the Bid inhibitor,[13] but neither the 12/15-LOX inhibitors nor the radical scavenger Trolox, could prevent tBid toxicity. These data strongly suggest that activation of 12/15-LOX and formation of ROS initiated cell death mechanisms after glutamate treatment, whereas activation of Bid, mitochondrial damage and the boost of ROS are hallmarks of downstream mechanisms that cannot be blocked by 12/15-LOX inhibitors or radical scavengers.

Both mitochondrial translocation of full-length Bid after the glutamate challenge and over-expression of tBid exerted similar effects on mitochondria and AIF-dependent cell death in the applied model system of HT-22 cells.[13] Here, we could not detect Bid cleavage after exposure to glutamate, suggesting that full-length Bid translocated to the mitochondria and/or only a small part of Bid was cleaved to tBid. This is in line with our previous observations[13] and reports by others[17] that suggested activation and mitochondrial translocation of full-length Bid before Bid cleavage and execution of mitochondrial death pathways. It is important to note that the Bid inhibitor prevented the translocation of activated full-length Bid and tBid to the mitochondria and the corresponding detrimental effects of mitochondria, suggesting that the effects of both forms of activated Bid on mitochondria are very similar. The exact mechanisms of Bid activation in the present model system are currently unknown and is a subject of ongoing studies.

A role for 12/15-LOX as an upstream trigger of mitochondrial execution mechanisms of cell death was further supported by analysis of mitochondrial morphology and AIF translocation after the glutamate challenge. Mitochondria are dynamic organelles that undergo permanent fission and fusion under physiological conditions. In damaged neurons, the disturbance of this dynamic process may lead to excessive fragmentation of mitochondria, thereby promoting cell death progression. Although the mechanisms controlling

mitochondrial morphology under pathological conditions are only partly known, increasing evidence suggests a potential role for oxidative stress and impaired bioenergetics as potential triggers of mitochondrial fission in the cell death program.[30–32] Here, we demonstrate that glutamate-induced cell death is associated with mitochondrial fission. Inhibition of 12/15-LOX prevented such glutamate-induced disruption of the mitochondrial morphology and also blocked the mitochondrial release of AIF to the nucleus. These data suggest that glutamate neurotoxicity involves enhanced mitochondrial fission that promotes the loss of mitochondrial integrity and progression of AIF-dependent cell death, and this process is triggered by glutamate-induced activation of 12/15-LOX. The translocation of AIF from mitochondria to the nucleus is a key feature of caspase-independent neuronal death as shown previously in models of glutamate toxicity,[10,13] OGD[10] and axonal stretch injury.[33] Upstream mechanisms of AIF release from mitochondria are not well understood but may involve activation of poly-(ADP-ribose)-polymerase-1[34] and calpains.[35] In addition, mitochondrial translocation of the BH3-only death agonists Bid,[10,13] Bim[36] and BNIP3[37] has been associated with AIF translocation in neurons. Here, the 12/15-LOX inhibitor PD146176 prevented AIF translocation to the nucleus, supporting a role for 12/15-LOX activation upstream of this mitochondrial mechanism of cell death. Notably, we also identified a therapeutic time window for interference with LOX activation in paradigms of neuronal cell death that may be relevant for therapeutic strategies in related neurological diseases. Recent work in models of cerebral ischemia exposed LOX as a potential target for neuroprotective strategies in stroke treatment.[38,39] In these studies, genetic 12/15-LOX deletion significantly reduced the infarct size in a mouse model of transient cerebral ischemia as compared with wild-type mice, and similar protective effects against ischemic brain damage were also achieved by treatment of wild-type mice with the LOX inhibitor baicalein.

In summary, our data identify 12/15-LOX as a key trigger in glutamate-induced oxidative stress that is initiated by GSH depletion, significantly amplified by Bid-dependent mechanisms of mitochondrial damage and executed by mitochondrial AIF release to the nucleus (Figure 8). The delineated sequences of glutamate-induced cell death signaling in HT-22 cells are highly relevant for neurodegenerative diseases and acute neurological disorders such as ischemic stroke or brain trauma, as these mechanisms have been identified as key features of neuronal death in related experimental models *in vitro* and *in vivo*.

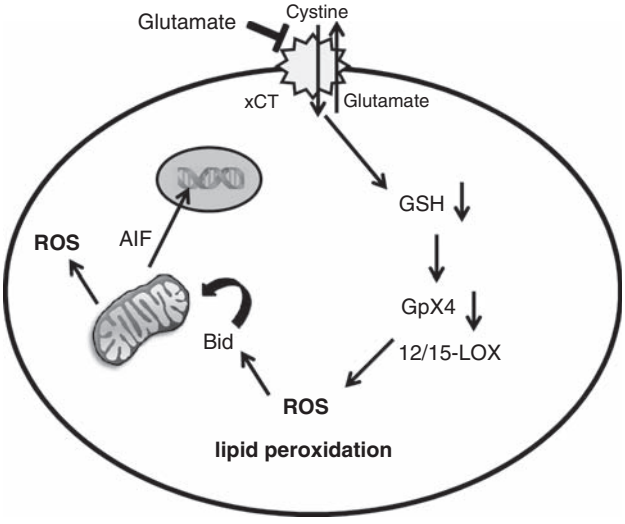

Figure 8 Overview on the mechanisms of glutamate-induced cell death in HT-22 cells. Glutamate induces glutathione depletion by inhibition of xc-transporters and consequently leads to GpX4 depletion and increased 12/15-lipoxygenase activity followed by an increase in lipid peroxides. This leads to Bid activation and mitochondrial damage followed by a second boost in ROS production and release of mitochondrial pro-apoptotic proteins such as AIF

Materials and methods

Cell culture and viability assays. HT-22 cells were cultured in Dulbecco's modified Eagle medium (DMEM, Invitrogen, Karlsruhe, Germany) supplemented with 10% heat-inactivated fetal calf serum, 100 U/ml penicillin, 100 μg/ml streptomycin and 2 mM glutamine. The LOX inhibitors PD146176 and AA861 (Sigma-Aldrich, Taufkirchen, Germany) were dissolved in DMSO (Sigma-Aldrich). PD146176 was diluted to a concentration of 50 mM and AA861 to a concentration of 10 mM, and these stock solutions were diluted with cell culture medium for each experiment up to final concentrations of 0.5 μM PD146176 and 0.1 μM AA861. Glutamate (2–5 mM) was added to the medium, and cell viability was evaluated 18 h later. Quantification of cell viability in HT-22 cells was performed in 96-well plates by MTT reduction at 0.25 mg/ml for 1.5 h. The reaction was terminated by removing the media and freezing the plate at -80°C for at least 1 h. Absorbance was then determined after solving the MTT dye in DMSO at 570 versus 630 nm (FluoStar, BMG Labtech, Offenburg, Germany). In addition, real-time detection of cellular viability was performed by measurements of cellular impedance by the xCELLigence system (Roche, Penzberg, Germany). For annexin-V/propidium iodide staining, HT-22 cells were cultured in 24-well plates and damaged with glutamate (3 and 5 mM). The cells were harvested 12–15 h after glutamate treatment by using Trypsin/EDTA, washed once in phosphate-buffered saline (PBS) and resuspended in binding buffer (PromoKine, Heidelberg, Germany). Propidium iodide and annexin-V-fluorescein isothiocyanate (FITC) were added at 1 μl/100 μl (PromoKine Annexin V-FITC Detection Kit) and incubated for 5 min at room temperature. Apoptotic and necrotic cells were detected using a FACScan (Becton, Dickinson and Company, Heidelberg, Germany). Annexin-V and propidium iodode fluorescence was exited at a wavelength of 488 nm. Emission was detected at 530 ± 40 nm for annexin-V and at 680 ± 30 nm for propidium iodide. In all, 10 000 cells per sample were collected.

Embryonic cortical cultures. Cortices were removed from embryonic day 16 Sprague–Dawley rats (Janvier, Le Genest St Isle, France) or Alox15-mice (Jackson Laboratory, Bar Harbor, ME, USA) and dissociated by trypsinization and trituation as followed: Isolated cortices were treated with trypsin (Sigma-Aldrich) (1 mg/ml) for 15 min at 37°C. The cortices were washed with Hank's balanced salt solution (HBSS) (made from 10 $\times$ HBSS, Invitrogen) and mixed with 1 mg/ml trypsin inhibitor (Sigma-Aldrich) and incubated for 2 min at room temperature. They were then washed two times with HBSS, and trituated in MEM + obtained from Eagle's minimum essential medium (Invitrogen) by addition of 1 mM HEPES (Biomol, Hamburg, Germany), 26 mM $NaHCO_3$, 40 mM glucose, 20 mM KCl, 1.2 mM L-glutamine (each Sigma-Aldrich), 1 mM sodium pyruvate (Biochrom, Berlin, Germany), 10% (v/v) fetal calf serum (FCS) (Invitrogen) and 10 mg/l gentamicin sulfate (Sigma-Aldrich). Cells were seeded in 35-mm culture dishes coated with polyethylenimine (Sigma-Aldrich). After 4 h the MEM + was replaced by Neurobasal medium (Invitrogen). Cells were treated on day 6 after preparation with 20 μM of glutamate. After 18–24 h the neurons were fixed with paraformaldehyde (4%) and stained with the fluorescent DNA-binding dye 4′,6-diamidino-2-phenylindole dihydrochloride (DAPI) (Sigma-Aldrich). Living and pyknotic cells were counted using a fluorescence microscope (Leica, Wetzlar, Germany) without knowledge of the treatment history. In total we counted 200 cells per cell culture dish ($n = 5$).

Plasmids and gene transfer. Plasmid pCDNA 3.1 + was obtained from Invitrogen. The tBid vector and control vectors were generated as previously

described.[29] For plasmid transfections 8×10^4 HT-22 cells were seeded in 24-well plates. The antibiotic-containing growth medium was removed and replaced with 900 μl antibiotic-free growth medium. Lipofectamine 2000 (Invitrogen) and ptBID plasmide or empty vector pCDNA 3.1 + were dissolved separately in OptiMEM I (Invitrogen). After 10 min of incubation at room temperature each DNA solution was combined with the respective volume of the Lipofectamine solution, mixed gently, and allowed to form plasmid liposomes for further 20 min at room temperature. The transfection mixture was added to the antibiotic-free cell culture medium to a final concentration of 1 μg DNA, and 1.5 μl/ml Lipofectamine 2000 in HT-22 cells. Controls were treated with 100 μl/ml OptiMEM only, and vehicle controls with 1.5 μl/ml Lipofectamine 2000.

Detection of oxidative stress. Intracellular ROS were detected by DCF. Within 6–17 h after glutamate treatment HT-22 cells were loaded with 1 μM CM-H2DCFDA (Invitrogen) for 30 min and fluorescence at 530 nm was monitored using a CyanTM MLE flow cytometer (DakoCytomation, Copenhagen, Denmark) at an excitation wavelength of 488 nm. For detection of cellular lipid peroxidation, cells were loaded with 2 μM BODIPY 581/591 C11 for 60 min in standard medium 6–17 h after glutamate treatment. Cells were then collected, washed and resuspended in PBS; flow cytometry was performed using 488 nm UV line argon laser for excitation and BODIPY emission was recorded on channels FL1 at 530 nm (green) and FL2 at 585 nm (red). Data were collected from at least 20 000 cells.

Immunocytochemistry. For immunocytochemistry, HT-22 cells were fixed with 4% PFA after their respective treatment. The cells were permeabilized by exposure for 5 min to 0.4% Triton X-100, and cells were placed in blocking solution (3% horse serum) for 30 min. Cells were then exposed to a polyclonal anti-AIF antibody (1 : 100 in block solution) overnight at 4°C, followed by incubation for 1 h with biotinylated anti-goat IgG antibody and 30 min in the presence of streptavidin Oregon Green 514 conjugate according to the manufacturer's protocol. The specificity of AIF immunoreactivity was controlled by omission of the primary antibody. Nuclei were counterstained with DAPI. Images were acquired using a fluorescence microscope.

Immunoblots. HT-22 cells were treated as described above. Nuclear and cytosolic extracts were obtained by using a Nuclear extraction kit (Active Motif, Rixensart, Belgium). For total cell protein extracts HT-22 cells were seeded in 24-well cell culture plates. At least four wells per condition were pooled. Cells were washed in PBS and lysed with 100 μl lysis buffer (Mannitol 0.25 M, Tris 0.05 M, EDTA 1 M, EGTA 1 M, DTT 1 mM, Triton-X 1% (all from Sigma-Aldrich), supplemented with 1 tablet per 10 ml Complete Mini protease inhibitor cocktail (Roche, Penzberg, Germany)). Protein extracts were kept on ice. To remove insoluble membrane fragments, extracts were centrifuged at 15 000 $\times$ *g* for 15 min at 4°C. The supernatants were stored at -80°C until further use. Western blot analysis was performed as previously described.[12] Briefly, the blot was probed with an anti-AIF goat polyclonal antibody (sc-9416, 1 : 1000, Santa Cruz Biotechnology, Santa Cruz, CA, USA) or anti-Bid (Cell signaling, Danvers, Massachusetts, USA) at 4°C overnight. Membranes were then exposed to the appropriate HRP-conjugated rabbit anti-goat secondary antibody (1 : 2500, Vector Laboratories, Burlingame, CA, USA) or anti-rabbit secondary antibody (1 : 2500, Vector Laboratories), followed by a chemiluminescence detection of antibody binding. Equal protein loading and purity of the extracts was controlled by re-probing the membrane with a monoclonal anti-α-tubulin antibody (T9026, 1 : 20 000, Sigma-Aldrich, data not shown) or an anti-HDAC1 antibody (Dianova, Hamburg, Germany; 1 : 1000). Chemidoc software (Bio-Rad, Munich, Germany) was used for quantification of western blot signals.

Statistical analysis. All data are given as means ± standard deviation (S.D.). For statistical comparisons between two groups Mann–Whitney *U*-test was used; multiple comparisons were performed by analysis of variance (ANOVA) followed by Scheffé's *post hoc* test. Calculations were performed with the Winstat standard statistical software package.

Conflict of interest

The authors declare no conflict of interest.

Acknowledgements. We thank the excellent technical support by Miriam Hoehn, Sandra Engel and Renate Hartmannsgruber. We also thank Dr. Cornelia Brendel, Thorsten Volkmann and Gavin Giel for the technical support with the FACS analyses, and Roche Applied Science for providing the xCELLigence System. Part of this work was supported by a grant from the Michael J Fox-Foundation to CC.

1. Culmsee C, Krieglstein J. Emerging pharmacotherapeutic strategies for the treatment of ischemic stroke. *Drug Discov Today Ther Strateg* 2006; **3**: 621–638.
2. Lo EH, Dalkara T, Moskowitz MA. Mechanisms, challenges and opportunities in stroke. *Nat Rev Neurosci* 2003; **4**: 399–415.
3. Culmsee C, Junker V, Kremers W, Thal S, Plesnila N, Krieglstein J. Combination therapy in ischemic stroke: synergistic neuroprotective effects of memantine and clenbuterol. *Stroke* 2004; **35**: 1197–1202.
4. Fisher M, Schaebitz W. An overview of acute stroke therapy: past, present, and future. *Arch Intern Med* 2000; **160**: 3196–3206.
5. Matsuda S, Umeda M, Uchida H, Kato H, Araki T. Alterations of oxidative stress markers and apoptosis markers in the striatum after transient focal cerebral ischemia in rats. *J Neural Transm* 2009; **116**: 395–404.
6. Murphy TH, Schnaar RL, Coyle JT. Immature cortical neurons are uniquely sensitive to glutamate toxicity by inhibition of cystine uptake. *FASEB J* 1990; **4**: 1624–1633.
7. Brennan AM, Suh SW, Won SJ, Narasimhan P, Kauppinen TM, Lee H *et al.* NADPH oxidase is the primary source of superoxide induced by NMDA receptor activation. *Nat Neurosci* 2009; **12**: 857–863.
8. Nagley P, Higgins GC, Atkin JD, Beart PM. Multifaceted deaths orchestrated by mitochondria in neurones. *Biochim Biophys Acta* 2010; **1802**: 167–185.
9. Liot G, Bossy B, Lubitz S, Kushnareva Y, Sejbuk N, Bossy-Wetzel E. Complex II inhibition by 3-NP causes mitochondrial fragmentation and neuronal cell death via an NMDA- and ROS-dependent pathway. *Cell Death Differ* 2009; **16**: 899–909.
10. Culmsee C, Zhu C, Landshamer S, Becattini B, Wagner E, Pellecchia M *et al.* Apoptosis-inducing factor triggered by poly(ADP-ribose) polymerase and Bid mediates neuronal cell death after oxygen-glucose deprivation and focal cerebral ischemia. *J Neurosci* 2005; **25**: 10262–10272.
11. Oppenheim RW, Blomgren K, Ethell DW, Koike M, Komatsu M, Prevette D *et al.* Developing postmitotic mammalian neurons in vivo lacking Apaf-1 undergo programmed cell death by a caspase-independent, nonapoptotic pathway involving autophagy. *J Neurosci* 2008; **28**: 1490–1497.
12. Plesnila N, Zhu C, Culmsee C, Groger M, Moskowitz MA, Blomgren K. Nuclear translocation of apoptosis-inducing factor after focal cerebral ischemia. *J Cereb Blood Flow Metab* 2004; **24**: 458–466.
13. Landshamer S, Hoehn M, Barth N, Duvezin-Caubet S, Schwake G, Tobaben S *et al.* Bid-induced release of AIF from mitochondria causes immediate neuronal cell death. *Cell Death Differ* 2008; **15**: 1553–1563.
14. Li Y, Maher P, Schubert D. A role for 12-lipoxygenase in nerve cell death caused by glutathione depletion. *Neuron* 1997; **19**: 453–463.
15. Murphy TH, Miyamoto M, Sastre A, Schnaar RL, Coyle JT. Glutamate toxicity in a neuronal cell line involves inhibition of cystine transport leading to oxidative stress. *Neuron* 1989; **2**: 1547–1558.
16. Seiler A, Schneider M, Forster H, Roth S, Wirth EK, Culmsee C *et al.* Glutathione peroxidase 4 senses and translates oxidative stress into 12/15-lipoxygenase dependent- and AIF-mediated cell death. *Cell Metab* 2008; **8**: 237–248.
17. Konig HG, Rehm M, Gudorf D, Krajewski S, Gross A, Ward MW *et al.* Full length Bid is sufficient to induce apoptosis of cultured rat hippocampal neurons. *BMC Cell Biol* 2007; **8**: 7.
18. Bannai S. Exchange of cystine and glutamate across plasma membrane of human fibroblasts. *J Biol Chem* 1986; **261**: 2256–2263.
19. de BS, Canals S, Casarejos MJ, Solano RM, Menendez J, Mena MA. Role of extracellular signal-regulated protein kinase in neuronal cell death induced by glutathione depletion in neuron/glia mesencephalic cultures. *J Neurochem* 2004; **91**: 667–682.
20. Khanna S, Roy S, Slivka A, Craft TK, Chaki S, Rink C *et al.* Neuroprotective properties of the natural vitamin E alpha-tocotrienol. *Stroke* 2005; **36**: 2258–2264.
21. Lin MT, Beal MF. Mitochondrial dysfunction and oxidative stress in neurodegenerative diseases. *Nature* 2006; **443**: 787–795.
22. Pallast S, Arai K, Wang X, Lo EH, van LK. 12/15-Lipoxygenase targets neuronal mitochondria under oxidative stress. *J Neurochem* 2009; **111**: 882–889.
23. Culmsee C, Landshamer S. Molecular insights into mechanisms of the cell death program: role in the progression of neurodegenerative disorders. *Curr Alzheimer Res* 2006; **3**: 269–283.
24. Plesnila N, Zinkel S, Le DA, Amin-Hanjani S, Wu Y, Qiu J *et al.* BID mediates neuronal cell death after oxygen/glucose deprivation and focal cerebral ischemia. *Proc Natl Acad Sci USA* 2001; **98**: 15318–15323.
25. Yin XM, Luo Y, Cao G, Bai L, Pei W, Kuharsky DK *et al.* Bid-mediated mitochondrial pathway is critical to ischemic neuronal apoptosis and focal cerebral ischemia. *J Biol Chem* 2002; **277**: 42074–42081.
26. Bermpohl D, You Z, Korsmeyer SJ, Moskowitz MA, Whalen MJ. Traumatic brain injury in mice deficient in Bid: effects on histopathology and functional outcome. *J Cereb Blood Flow Metab* 2006; **26**: 625–633.

27. Becattini B, Culmsee C, Leone M, Zhai D, Zhang X, Crowell KJ *et al.* Structure-activity relationships by interligand NOE-based design and synthesis of antiapoptotic compounds targeting Bid. *Proc Natl Acad Sci USA* 2006; **103**: 12602–12606.
28. Culmsee C, Plesnila N. Targeting Bid to prevent programmed cell death in neurons. *Biochem Soc Trans* 2006; **34**: 1334–1340.
29. Kazhdan I, Long L, Montellano R, Cavazos DA, Marciniak RA. Targeted gene therapy for breast cancer with truncated Bid. *Cancer Gene Ther* 2006; **13**: 141–149.
30. Cho DH, Nakamura T, Fang J, Cieplak P, Godzik A, Gu Z *et al.* S-nitrosylation of Drp1 mediates beta-amyloid-related mitochondrial fission and neuronal injury. *Science* 2009; **324**: 102–105.
31. Knott AB, Perkins G, Schwarzenbacher R, Bossy-Wetzel E. Mitochondrial fragmentation in neurodegeneration. *Nat Rev Neurosci* 2008; **9**: 505–518.
32. Yuan H, Gerencser AA, Liot G, Lipton SA, Ellisman M, Perkins GA *et al.* Mitochondrial fission is an upstream and required event for bax foci formation in response to nitric oxide in cortical neurons. *Cell Death Differ* 2007; **14**: 462–471.
33. Slemmer JE, Zhu C, Landshamer S, Trabold R, Grohm J, Ardeshiri A *et al.* Causal role of apoptosis-inducing factor for neuronal cell death following traumatic brain injury. *Am J Pathol* 2008; **173**: 1795–1805.
34. Yu SW, Wang H, Poitras MF, Coombs C, Bowers WJ, Federoff HJ *et al.* Mediation of poly(ADP-ribose) polymerase-1-dependent cell death by apoptosis-inducing factor. *Science* 2002; **297**: 259–263.
35. Polster BM, Basanez G, Etxebarria A, Hardwick JM, Nicholls DG. Calpain I induces cleavage and release of apoptosis-inducing factor from isolated mitochondria. *J Biol Chem* 2005; **280**: 6447–6454.
36. Gao Y, Signore AP, Yin W, Cao G, Yin XM, Sun F *et al.* Neuroprotection against focal ischemic brain injury by inhibition of c-Jun N-terminal kinase and attenuation of the mitochondrial apoptosis-signaling pathway. *J Cereb Blood Flow Metab* 2005; **25**: 694–712.
37. Xu X, Chua CC, Kong J, Kostrzewa RM, Kumaraguru U, Hamdy RC *et al.* Necrostatin-1 protects against glutamate-induced glutathione depletion and caspase-independent cell death in HT-22 cells. *J Neurochem* 2007; **103**: 2004–2014.
38. van LK, Kim HY, Lee SR, Jin G, Arai K, Lo EH. Baicalein and 12/15-lipoxygenase in the ischemic brain. *Stroke* 2006; **37**: 3014–3018.
39. van LK, Arai K, Jin G, Kenyon V, Gerstner B, Rosenberg PA *et al.* Novel lipoxygenase inhibitors as neuroprotective reagents. *J Neurosci Res* 2008; **86**: 904–909.

Supplementary Information accompanies the paper on Cell Death and Differentiation website (http://www.nature.com/cdd)